G. Demofonti and L. Rizzi†*

Experimental Evaluation of CTOA in Controlling Unstable Ductile Fracture Propagation

REFERENCE Demofonti, G. and Rizzi, L., **Experimental evaluation of CTOA in controlling unstable ductile fracture propagation**, *Defect Assessment in Components – Fundamentals and Applications*, ESIS/EGF9 (Edited by J. G. Blauel and K.-H. Schwalbe) 1991, Mechanical Engineering Publications, London, pp. 693–703.

ABSTRACT Recent literature works have discussed the introduction of the crack tip opening angle, CTOA, as a post-yielding fracture mechanics parameter, for assessing the ductile crack propagation in gas transmission pipelines of large diameters (36–56 inches). Nevertheless the practical use of the CTOA is still limited, because further extensive experimental work is necessary.

In this paper the *R* curve and the driving-force curve have been expressed in terms of CTOA, as a function of the crack length, and the unstable crack propagation condition is given by

$$(\mathrm{CTOA})_{\mathrm{applied}} > (\mathrm{CTOA})_{\mathrm{material}}$$

In this case the intersection of the $(\mathrm{CTOA})_{\mathrm{material}}$ curve (*R* curve) and the $(\mathrm{CTOA})_{\mathrm{applied}}$ curve (driving-force curve) provides a theoretical value of unstable crack growth, Δa_{th}.

Laboratory fracture propagation tests have been carried out with the aim of comparing such theoretical values, Δa_{th}, with the actual crack lengths, Δa_{real}.

In order to obtain different driving forces, a 'spring bar' device has been developed and established.

The experimental tests have been performed on pipelines steels with different toughness values.

The theoretical values of CTOA compared with the actual values, directly measured on the specimen fracture surface confirm the reliability of the $(\mathrm{CTOA})_{\mathrm{mat}}$, as a post-yielding fracture mechanics parameter.

Introduction

Nowadays gas companies tend to use the highest grade steels (API X70 or more) for large diameter (36–56 inches) gas transmission lines. In fact when good field weldability and high nominal toughness are combined with high yield strength, higher operating pressures can be adopted for a given thickness.

This situation has been made possible by the introduction of new classes of microalloyed commercial steels and more advanced rolling practices involving thermomechanical treatment such as controlled rolling (CR) and/or controlled rolling followed by accelerated cooling (AC) **(1)–(3)**.

However, recent experience has clearly shown that where high-grade pipes are concerned, the problem of unstable longitudinal ductile fracture propagation must not be treated lightly **(4)–(6)**.

Indeed, though on the one hand there exist high grade pipes of high toughness capable of rapidly arresting such a fracture, on the other hand, as these

* Centro Sviluppo Materiali Spa, Via di Castel Romano 100-102, 00129 Rome, Italy.
† ILVA, Taranto Works, Rome, Italy.

toughness values, expressed in terms of Charpy 'V' energies, are particularly high (over 200 J/cm^2) they cannot really be proposed as production standards in many cases.

It is thus necessary to know (and hence control) the various parameters that govern the phenomenon and fracture arrest/propagation conditions in general.

One new way of tackling the problem is to develop a physical propagation model capable of adequately describing the complex system of interaction existing between a plastically-deforming bursting pipe and the surrounding environment. This approach, though demanding, is feasible, because of the availability of very considerable computing capacity (in terms of computers and codes) and a great amount of experimental data on fracture propagation in gas transmission lines (much of which derived from numerous full-scale bursting tests) **(7)(8)**.

More specifically it can be said that ductile fracture propagation on a gas transmission line is controlled essentially by an energy balance between the action of the gas which issues from the pipe (driving force) and the resisting action, offered by the surrounding backfill and the intrinsic toughness of the steel.

Regarding this last point, in particular, the use of fracture criteria based on fracture mechanics concepts combined with plastic deformations seems particularly promising. This is because the deformations are intrinsically bound up also with the configuration of the pipe during the fracture process and hence, in final analysis, to the maximum work the gas can do. The crack tip parameter applicable to such viscoplastic dynamic conditions as exist in ductile fracture propagation in gas pipelines is not at present definitively established. However, a number of workers **(9)–(13)** have argued from both theoretical and experimental work that crack tip opening angle (CTOA) may be an appropriate crack tip parameter. If CTOA (defined as the angle at which the two new fracture surfaces emerge from the crack tip) is adopted as a toughness parameter of the steel, it can be measured in the laboratory on small specimens **(14)(15)**.

In the research concerned, laboratory tests have been run to ascertain the real validity of the R curve (expressed in terms of CTOA) as the post-yielding fracture mechanics parameter, capable of characterising the behaviour of a steel as regards fracture propagation. This has been done by utilising the geometric definition of the CTOA and an appropriate system of spring bars, dimensioned to provide the driving force necessary for the experimentation.

Analytical approach

Unstable crack propagation conditions, expressed in terms of deformation (crack tip opening displacement – CTOD) can be written generally as

$$\mathrm{d}/\mathrm{d}a(\mathrm{CTOD})_{\mathrm{appl}} > \mathrm{d}/\mathrm{d}a(\mathrm{CTOD})_{\mathrm{mat}}$$

where

a = crack length
mat = parameters characteristic of the steel (R curve)
appl = parameters applied by loading system (driving-force curve).

Using the assumptions of the kinematic approach this formulation can be transformed so that the instability condition is expressed in terms of crack tip opening angle.

The principal assumption of the kinematic approach is

$$\mathrm{CTOA} = 2\gamma_{\mathrm{p}} = 2 \arctan\left(1/2 \lim_{\Delta a \to 0} \frac{\Delta \delta t}{\Delta a}\right)$$

The parameter being defined as in Fig. 1(a).

Using this assumption the CTOD instability condition becomes

$$(\mathrm{CTOA})_{\mathrm{appl}} > (\mathrm{CTOA})_{\mathrm{mat}} \qquad (1)$$

The scope of this paper is to detail an experimental verification of this condition. Three point bending (TPB) specimens of various steels for pipelines guaranteeing diverse initiation and crack arrest conditions were used.

Measurement of the R curve in terms of CTOA and calculation of the driving force curve (applied CTOA) have been effected by employing the definition of the crack tip opening angle given by the kinematic approach **(14)(15)**.

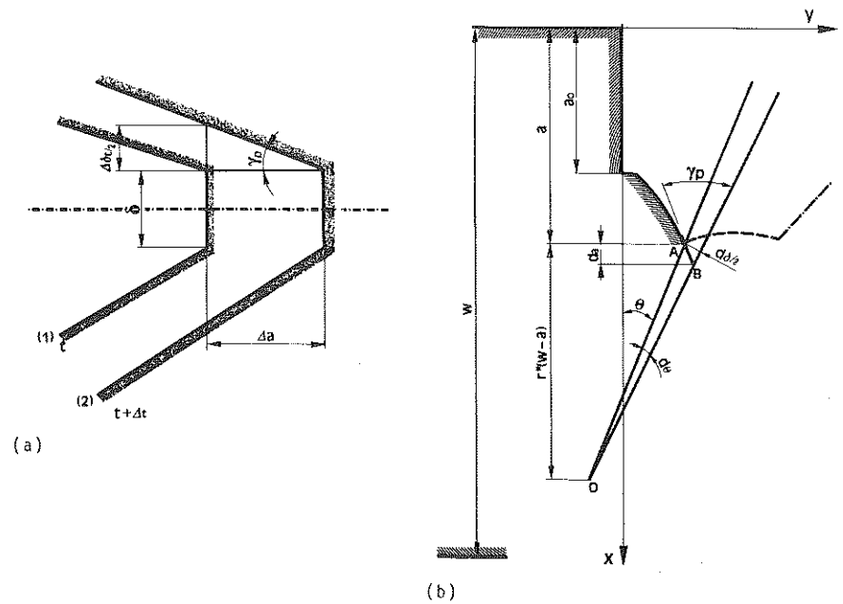

Fig 1 Geometric schematisation utilised in definition and measurement of crack tip opening angle (CTOA)

To perform such analysis, a second fundamental assumption is introduced and a number of geometric relationships established. Referring to Fig. 1(b), the second assumption is that: "In fully plastic conditions the two parts of a specimen already intersected by the fracture, in a bending test, for instance, rotate as rigid bodies around a centre of instantaneous rotation 'O' which is located on the symmetry axis at a distance r^* $(w - a)$ from the crack tip; 'a' is the crack length and $r^* \simeq 0.45$ for TPB specimen, and is constant during the crack propagation".

From this assumption, geometric considerations (Fig. 1(b); $\overline{AB} = da/\cos(\gamma_p - \Theta)$; $\overline{OA} = r^*(w - a)/\cos\Theta$) allow the formulation of the following relation between $(CTOA)_{mat}$ and the rotation 2Θ experienced by one half of the test piece relative to the other

$$\frac{d\Theta}{da} = \frac{\sin \gamma p \cos \Theta}{\cos(\gamma p - \Theta) r^*(w - a)}$$

or rearranging with the form of the expression to render γp explicit

$$\{CTOA(a)\}_{mat} = 2\gamma_P = 2 \arctan \left\{ r^*(w - a) \frac{d\Theta}{da} \cdot \left(1 - r^*(w - a) \frac{d\Theta}{da} \tan \Theta\right)^{-1} \right\} \tag{2}$$

or in simplified form

$$\{CTOA(a)\}_{mat} = 2 \arctan \left\{ r^*(w - a) \frac{d\Theta}{da} \right\} \tag{3}$$

where (with reference to Fig. 2 which illustrates the exact geometry of the specimen utilised in the experimentation) w is the total height of specimen.

It is clear that the assumption of plane strain conditions lies at the basis of such a geometric treatment of the problem.

Starting from the experimental curve $\Theta = \Theta(a)$, it is easy to determine the $\{CTOA\}_{mat} = \{CTOA(a)\}_{mat}$ curve, using equation (2) or more simply equation (3). The experimental curve $\Theta = \Theta(a)$ in this work is obtained from measurements of photographs taken during the propagation of the crack.

As regards the $\{CTOA(a)\}_{appl}$ curve applied by the system on the specimen – the Driving Force – this sums to be a function both of the specimen dimensions, and the compliance of the load system (machine, specimen, and clamps). Its value can be obtained by geometric methods in the following way.

During the unstable propagation phase the following relationship is verified instant by instant **(16)**

$$d(\Delta_{EL}) + d(\Delta_{PL}) + d(\Delta_M) \leqslant 0 \tag{4}$$

which indicates all the vertical movements of the specimen deflection, during the propagation phase, and relative to the axis of symmetry. The various

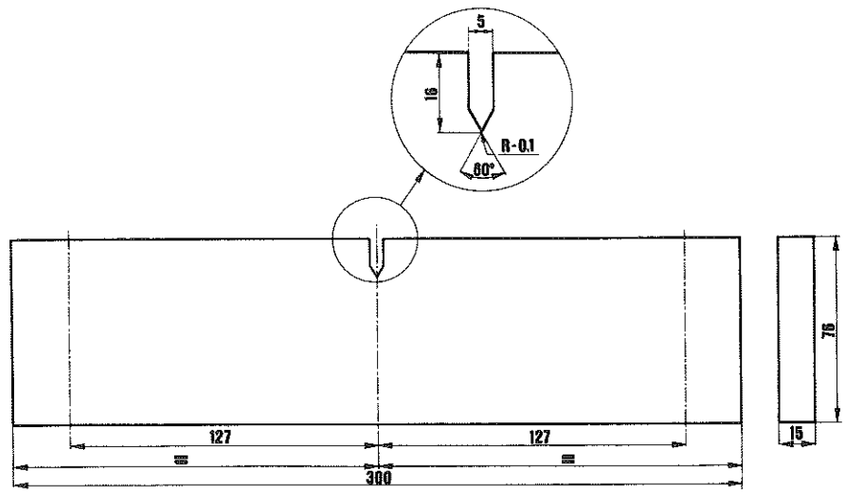

Fig 2 Geometry of TPB specimen used

movements are

Δ_{EL} = elasticity of specimen
Δ_{PL} = plastic deformation of specimen
Δ_M = displacement of the load system

With specific reference to the TPB specimen in Fig. 2, the three terms can be expressed as

$$\Delta_{EL} = \frac{2P}{EB} \cdot \frac{S^3}{(w - a)^3} \tag{5}$$

$$\Delta_{PL} = S \tan \Theta \tag{6}$$

$$\Delta_M = C \cdot P \tag{7}$$

where

C is the compliance of the machine,
E the modulus of elasticity of the steel,
S half span of specimen.

The load P, under conditions of full plasticity of ligament, can be expressed as a limit load P_L equal to

$$P_L = 0.7\sigma_0 \frac{B}{S}(w - a)^2 \tag{8}$$

where

σ_0 = flow stress of steel
B = thickness of test piece

Utilising this limit load expression, for derivation of expressions (5), (6), and (7) with respect to crack length, the inequality (4) can be written in the following way

$$1.4\,\frac{\sigma_0}{E}\,\frac{S^2}{(w-a)^2} - 1.4\,\frac{\sigma_0}{S}\,BC(w-a) + S\,\frac{d\Theta}{da}\,\frac{1}{\cos^2\Theta} \leqslant 0 \qquad (9)$$

Rendering this in explicit terms of $d\Theta/da$ and utilising equation (3), the expression of the applied CTOA, as a function of crack length, is the following

$$\{\mathrm{CTOA}(a)\}_{\mathrm{appl}} = 2 \arctan \left[0.63\sigma_0(w-a)\left\{\frac{BC(w-a)}{S^2} - \frac{S}{(w-a)^2E}\right\}\cdot\cos^2\Theta\right] \qquad (10)$$

Equation (10) is the desired relation; it clearly indicates how the applied CTOA depends on compliance of the machine and the configuration assumed by the specimen.

Experimental

The following steps were involved in the experimental verification of the unstable propagation conditions of a crack that can be predicted by comparison of the R curve and the driving-force curve furnished by equation (10):

- development of an adequate spring bar system;
- selection and characterisation of a suitable set of materials;
- experimental check of instability conditions.

Development of spring bar system

An adequate spring bar system was developed and built in order to increase the compliance of the load system and hence the driving force supplied. The system consists of four simply-supported beams of uniform strength, stressed by bending. By an appropriate combination of support positions it was possible to obtain in three different configurations (whose characteristics are reported in Table 1), and the capacity to absorb sufficient elastic energy to ensure unstable crack propagation.

Selection and characterisation of materials

Linepipe steels ranging from API X60 to X80 in grade were selected for the experimentation. All were commercial products, some of which had been subjected to controlled rolling and others to controlled rolling followed by accelerated cooling. For additional details and chemical composition refer to reference **(17)**.

Table 1 Characteristics of spring bar system

Spring bar geometry	*Max. load (kN)*	*Compliance (mm/kN)*
A	149.6	0.269
B	149.6	0.172
C	196.2	0.139

Table 2 Mechanical properties of the steels used

Steel	*Rs (MPa)*	*UTS (MPa)*	*Cv (J/cm²)*	*Average CTOA (degrees)*
413 (AC)	500	649	208	10
421 (AC)	536	646	147	8
494 (AC)	504	627	162	8
7/63 (CR)	528	632	125	7.6
12 (AC)	554	634	285	12
35 (CR)	511	623	152	8.5
NB2 (CR)	486	622	125	8.6

Table 2 indicates the yield strength (Rs) and UTS, together with Charpy 'V' energy values and the 'plateau' CTOA value (this being the mean of the $\mathrm{CTOA}_{\mathrm{mat}}$ values occurring in the 'plateau' of CTOA verses crack growth curve) obtained during propagation.

The $\{\mathrm{CTOA}\}_{\mathrm{mat}} = \{\mathrm{CTOA}(a)\}_{\mathrm{mat}}$ curve was measured for each steel, utilising the curve $\Theta = \Theta(a)$.

By way of example, Fig. 3 illustrates two of these curves, namely those for steels 35 and 12. As already reported **(14)(15)**, the $\{\mathrm{CTOA}(a)\}_{\mathrm{mat}}$ curve of the steel decreases from high values near the initiation phase and then stabilises at a virtually constant 'plateau' value in the propagation phase.

In the same figures are presented three analytically derived curves of the applied CTOA which defines the crack driving force. The curves (A, B, C) are relevant to three different configurations of the spring bar loading system.

Experimental check of instability conditions

By reference to the curves illustrated in Fig. 3, it is possible to establish the zone in which the relationship

$$(\mathrm{CTOA})_{\mathrm{mat}} < (\mathrm{CTOA})_{\mathrm{appl}}$$

is satisfied for each of the various steels considered.

This indicates where unstable crack propagation is possible for a certain length of ligament, and hence the arrest thereof.

Thus steel 12 exhibits three different possible types of crack advance. If loaded under configuration C only, stable propagation is possible; under configuration B, a brief period of stable propagation is followed by unstable propagation and then arrest; while when loaded in configuration A, unstable propagation is followed by crack arrest.

A series of experimental tests has been performed by appropriate use of the spring bar configurations available to verify these predictions.

Comparison of measured and predicted crack advance values is illustrated in Fig. 4.

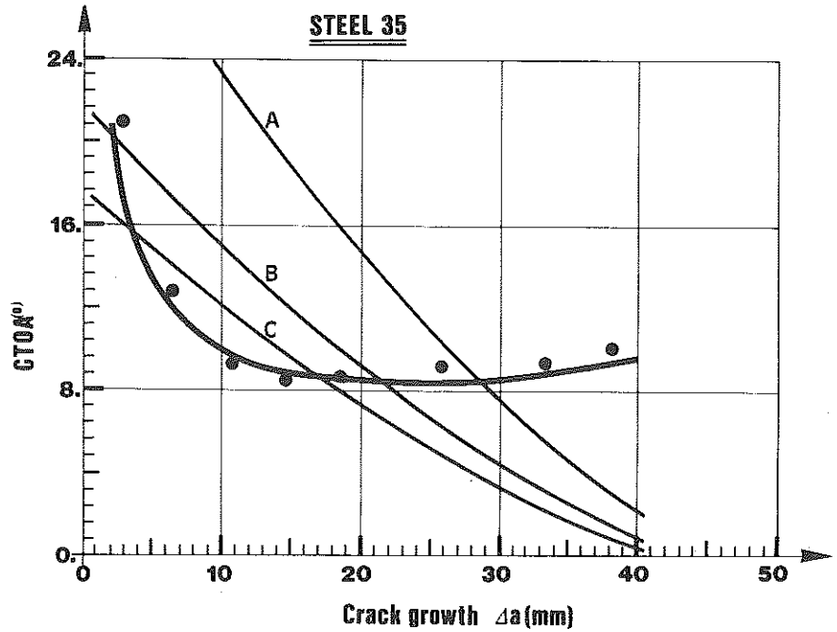

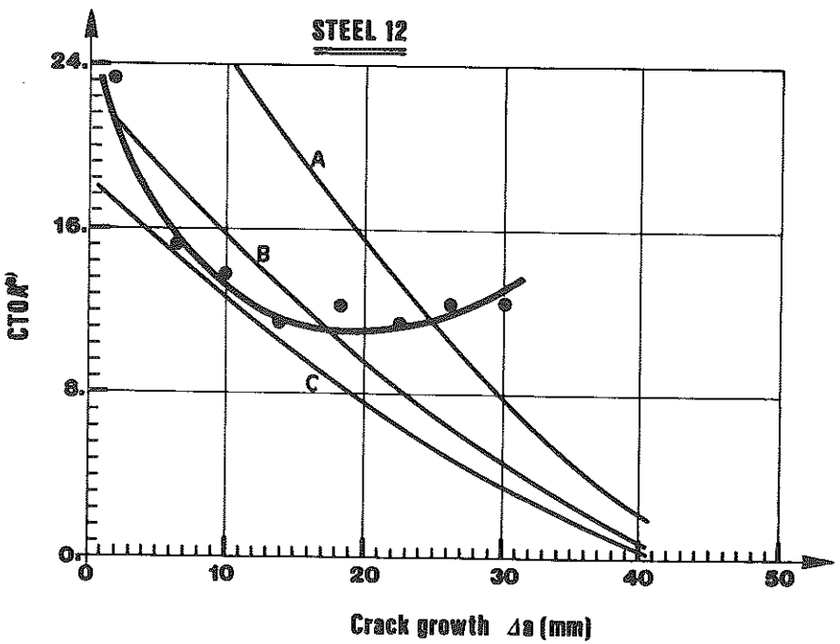

Fig 3 *R* **curves expressed in terms of CTOA, together with applied CTOA curves for comparison**

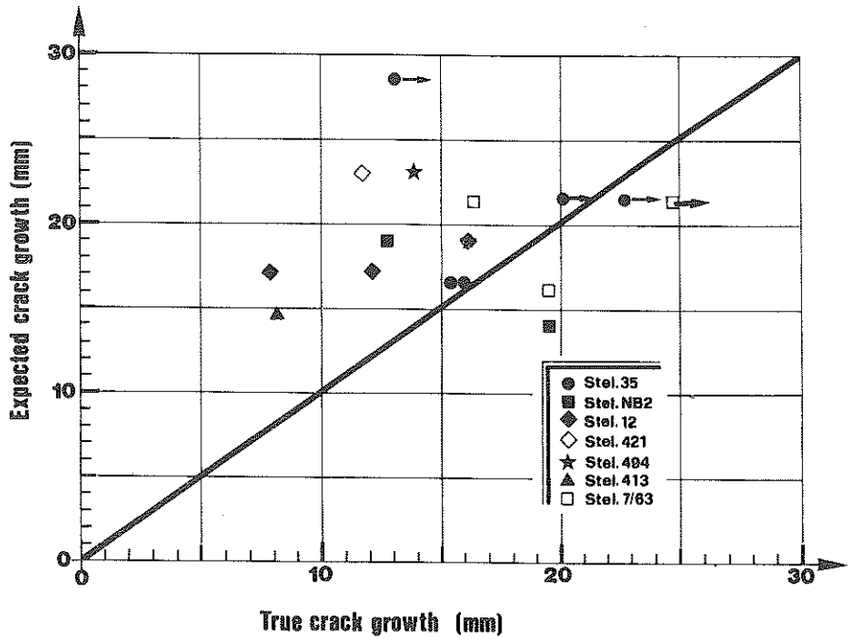

Fig 4 Comparison of length of crack of unstable propagation actually measured and that predicted on the basis of the *R* curve

In some instances, indicated by an arrow, propagation occurred in plane strain in an initial stretch, and then continued in shear mode (plane stress) up to complete rupture of the specimen. In this case, which was the most frequent result for steel 35, the length of the crack relative to plane strain advance is reported on the graph.

Analysis of experimental results

The experimental results indicate the following:

- in the cases examined, the initiation of unstable crack propagation is generally correctly predicted;
- the calculated length of the stretch affected by unstable crack propagation is greater (about 20 percent, on average) than that which actually occurs;
- in four of the seventeen cases examined, the fracture affected the whole ligament, contrary to expectations.

As aready indicated, this latter case is associated with a change in the fracture plane which rotates by 45 degrees. This may be due to the extensive field of plastic deformation associated with the punch which is different from one steel to another. This idea is supported by the consideration that this event

tended to occur somewhat repeatedly in only one of the steels examined, and always after plane strain crack propagation over a sufficiently long stretch. It should be recalled, however, that the basic assumption adopted for the analytical/experimental approach is that the fracture occurs in plane strain.

More generally, within the framework of this assumption, it can be said that the results are in line the proposed 'model', and in the majority of cases they are conservative, the prediction almost always being for the propagation of longer cracks than actually occurred. That is in the majority of cases crack arrest in the experimental tests occurred before the prediction.

In this regard, it is held that in addition to indecision on measurements, a possible cause of this may also be failure to consider the friction effect. This effect, of course, reduces the energy made available to break the specimen and hence the driving force of the system.

Conclusions

The experimental results presented have provided a better understanding of the representativeness, and hence the applicability, of a post-yielding fracture mechanics parameter, such as the crack tip opening angle. The following conclusions can be drawn.

(1) The crack tip opening angle actually represents a useful fracture mechanics parameter for the study and control of unstable ductile crack propagation of the type that may occur in a large-diameter gas transmission line. This is borne out by the general agreement between the unstable crack propagation values predicting by utilising $\{\mathrm{CTOA}\}_{\mathrm{mat}}$ as the critical parameter, and those obtained experimentally on three point bending specimens in a spring bar system.
(2) The purely geometric approach adopted in the work for defining and measuring the crack tip opening angle is parricularly useful and is suitable for a full 'description' of ductile fracture propagation on a bending specimen.
(3) Further work is needed for a better understanding of factors governing the crack tip opening angle.

Acknowledgement

A special thanks to Dr I. Cole for contribution to the discussion.

References

(1) DUNEN, D. P. and CHANDRA, T. (Editors) (1984) *High strength low alloy steels*, AIME, New York.
(2) SOUTHWICK, P. D. (Editor) (1985) *Accelerated cooling of steel*, AIME, New York.
(3) GRAY, J. M., *et al.* (Editors) (1985) *HSLA steels metallurgy and applications*, ASM, Cleveland, OH.
(4) VENZI, S., *et al.* (1985) Sixth NG-18/EPRG Biennial Tech. Meeting, Camogli, Italy, p. 139.
(5) RE, G., *et al.* (1988) Seventh NG-18/EPRG Biennial Technical Meeting, Calgary, paper No. **15**.

(6) BUZZICHELLI, G., *et al.* (1988) Seventh NG-18/EPRG Biennial Technical Meeting, Calgary, paper No. **10**.
(7) KANNINEN, M., *et al.* (1987) Int. Conf. Pipe Technology, AIM, Cleveland, OH, pp. 453–472.
(8) BONOMO, F., *et al.* (1985) The Third Int. Conf. on Steel Rolling, AIM, Cleveland, OH, pp. 560–567.
(9) SHIH, G. F., *et al.* (1979) *ASTM STP 668*, ASTM, Philadelphia, pp. 65–119.
(10) OGASAWARA, M. (1983) *Engng Fracture Mech.*, **18**, 839–849.
(11) AIHARA, S., *et al.* (1981) *Advances in fracture research*, Pergamon Press, Oxford, p. 2329.
(12) HOFF, R., *et al.* (1987) *Engng Fracture Mech.*, **26**, 445–461.
(13) KOBAYASHI, T., *et al.* (1989) *J. Mech. Phys Solids*, **37**, 759–777.
(14) VENZI, S., *et al.* (1981) *Analytical and experimental fracture mechanics* (Edited by G. C. Sih and M. Mirabile), Sijthoff and Noordhoff, The Netherlands, p. 737.
(15) DEMOFONTI, G., *et al.* (1988) Proc. XXII Meeting AIM, AIM, Cleveland, OH, pp. 1043–1059.
(16) PARIS, P. C., *et al.* (1979) *ASTM STP 668*, ASTM, Philadelphia, pp. 5–36.
(17) DEMOFONTI, G. (1989) ECSC Report n. 7210-KE/412, Dic.